

Land Cover Clustering based on Improved Dictionary Learning Method from Modis Data

Mariem Zaouali, Sonia Bouzidi and Ezzeddine Zagrouba

¹RIADI Laboratory, Research Team on Intelligent Systems in Image and Artificial Vision, ISI,
University of Tunis El Manar, Tunis, Tunisia

Keywords: k-Means Clustering Algorithm, Discriminative Temporal Behavior, Dictionary Learning, Coarse Spatial Resolution Images, Remote Sensing, Sparse Representation.

Abstract: An approach based on k-means clustering algorithm combined with the concept of sparse representation is proposed in this paper. We intend to discriminate, each vegetation type, by its temporal behavior. Our method is composed of two main parts : The first part consists of designing the dictionary that we are going to use. For this reason, we propose a modification of the k-svd algorithm by switching the use of OMP algorithm by the SunSAL algorithm. Then we carry on an unsupervised clustering process using k-means algorithm on sparse vectors. As a result, we found that SunSAL algorithm outperforms the OMP algorithm and we succeed to elaborate discriminative temporal behaviors of the vegetation in our region of study. As perspectives, our approach could be considered as an attempt to overcome the shortage of high spatial resolution data since we are relying only on coarse remote sensing images like MODIS to monitor Land Cover dynamics.

1 INTRODUCTION

Over the past decades, remote sensing measurements have played a key role in analyzing climate changes and dynamics of ecosystem, in order to protect the Earth surface from environmental disasters. Nowadays, thanks to the development of aerospace technologies, a great number of satellite sensors has been launched, which has increased incredibly the amount of available data. The use of multitemporal coarse resolution satellite imagery has shown potentials but requires a considerable amount of data, especially ground truth, to monitor land cover change (Zhan et al., 2002; Morton et al., 2005). Thus, unsupervised methods give a more attractive solution to that. In this work, we explore a coarse spatial resolution data but highly frequent in time. We estimate that the temporal features is interesting to model the land cover and could improve vegetation cover classification (Jia et al., 2013). Indeed, time series vegetation index (eg. NDVI or EVI) are approved to well describe vegetation growth as well as revealing the vegetation type information since it represents the phenology cycle (Brown et al., 2013). Whereas, the main issue comes to how surpass dimensionality of time series data and limited availability of labeled samples to improve land cover classification accuracy. In a recent work (Yang et al., 2014), an approach is pro-

posed based on NDVI, PCA and ISODATA clustering algorithm (which groups pixels with similar spatial and spectral characteristics into classes (Mohamady et al., 2015)). However, in practical application, the quality of this classification is often not enough (Guha and Ward, 2012). Recently, sparse modeling has proven fruitful application in various fields such as signal, image, compression and others (Lim et al., 2012; Mahmoudi and Sapiro, 2012; Wright et al., 2009). It also provides a useful tool for machine learning. In fact, sparse representation can classify any samples based on the concept that it is a linear combination of labeled prototype samples (Chen and Donoho, 1994). In this work, we tried to exploit sparse representation paradigm since it is a tool for dimensionality reduction, in order to conduct unsupervised clustering. The idea is to find a dictionary that can well approximate NDVI temporal behavior without the requirement of labeled samples. The final result is a discriminant temporal behavior of each land cover and a labeled data. This paper is organized as follows: Section II presents Related concepts, Section III describes the proposed approach, Section IV presents the Study area, Section V describes experimental protocol and results. Finally the last Section is the conclusion.

2 RELATED CONCEPTS

Sparse representation helps having compact representation of images by using a reduced set of coefficients from a basis of elements, i.e dictionary, which is a matrix whose columns d_k are called atoms. This technique has been applied in various fields including remote sensing. In our case, we want to exploit sparse representation in order to improve land cover classification and then use it for changes detection. We aim to discriminate classes by their temporal behavior in order to make detecting changes easier. This would be an attempt to deal with limited availability of labeled samples. Our approach is based on considering temporal patches as dictionary atoms This means that we track the temporal behavior of a pixel through the time series images. In this section, we present the definition of sparse representation and its classifier logic.

2.1 Sparse Representation

Let the dictionary $\mathbf{D} \in \mathbb{R}^{n \times p}$ be a base containing \mathbf{p} atoms, , each one composed of \mathbf{n} rows, with $n < p$. This dictionary contains a set of temporal behaviors chosen randomly from the study area. For a given signal \mathbf{Y} , it is demanded to find a sparse vector \mathbf{X} , having only few non zeros coefficients, combining linearly the atoms of dictionary \mathbf{D} . This problem could be presented in equation 1:

$$\arg \min \|\mathbf{X}\|_0 \text{ subject to } \|\mathbf{Y} - \mathbf{DX}\|_2 \leq \delta \quad (1)$$

with \mathbf{Y} is the signal to represent via \mathbf{X} from \mathbf{D} and δ is the level of sparsity. Due to the presence of possible modeling error and noise, equation (1) is often replaced by

$$\arg \min \|\mathbf{X}\|_1 \text{ subject to } \|\mathbf{Y} - \mathbf{DX}\|_2 \leq \delta \quad (2)$$

where $\|\mathbf{X}\|_1 = \sum_{i=1}^n |x_i|$. This is due to the difficulty to resolve l_0 norm, which is considered as NP-hard problem. In fact, several algorithms have been proposed to solve equation (1) such as Basis pursuit BP (Chen and Donoho, 1994), Orthogonal Matching Pursuit OMP (Tropp et al., 2007) and Sparse UNmixing by variable Splitting and Augmented Lagrangian SunSAL (Bioucas-Dias and Figueiredo, 2010). BP replaces the l_0 norm with l_1 norm as mentioned in equation (2). However, OMP proposes a greed strategy. In the first iteration, OMP takes the test sample \mathbf{Y} as an initial residual, then, through each iteration, OMP has to recognize the atom that could best approximate the residual. Using the selected atoms, OMP re-estimates \mathbf{X} . This algorithm will stop once if one of the following conditions are met: Approximation error is less than a certain threshold or a predefined number

of atoms have been selected. However SunSAL proposes another approach. It is based on the fact that the equation (1) is equivalent to the following unconstrained optimization problem:

$$\min \frac{1}{2} \|\mathbf{y} - \mathbf{Dx}\|_2^2 + \lambda \|\mathbf{x}\|_1 \quad (3)$$

where λ is a Lagrangian multiplier. SunSAL provides an efficient solution form $l_2 - l_1$ norm problem. It is considered more efficient and less complex with equal accurate solution as an alternate of LASSO-(least absolute shrinkage and selection operator)(Xue et al., 2015). In this work, we deal with OMP and SunSAL and compare their performance in designing dictionary. In next section, we describe how, with the help of dictionary and sparse representation, we can classify training samples.

2.2 Sparse Representation based Classifier

Sparse representation relies on the idea that any signal is a linear combination of atoms belonging to a class. That is mean that any signal representing a class C_i could be sparsely composed by remarkable coefficient of class C_i while for the other class, are barely zeros. Indeed, for a set of k objects of classes : $v_{i,1}, \dots, v_{i,k}$ with $v_{i,j}$ is the j^{th} sample of the i^{th} class, let consider $D_i = [v_{i,1}, \dots, v_{i,k}]$ as the matrix representing the i^{th} . Let $\mathbf{D} = [D_1, D_2, \dots, D_p]$ be a dictionary. The resolution of $\mathbf{Y} = \mathbf{DX}$ with $\mathbf{X} = [0, \dots, 0, x_{i,1}, x_{i,2}, \dots, x_{i,j}, 0, \dots, 0]^T$ is the sparse vector, gives us the label of the sample Y . In fact X would have only few non zero coefficients which refer to the class of Y . Thanks to the residual base criterion formula :

$$\text{class}(y_i) = \arg \min_{j \in 1 \dots c} \|\mathbf{Y} - \mathbf{DX}\|_2 \quad (4)$$

where $\text{class}(y_i)$ is the class label affected to y , we can measure the accuracy of the classification result. In our case, we cannot determine the label of samples y_i because the dictionary atoms' are anonymous. They just were extracted from the study region without any further information pertaining to its type. The proposed solution to this point, is described in the next section.

3 PROPOSED APPROACH

In this work, we try to classify vegetation based on its discriminant behavior using NDVI (Normalized Differential Vegetation Index) profiles. This index is defined as the difference between the visible (red) and

near-infrared (nir) bands, over their sum. It is directly related to the amount of photo synthetically-active radiation intercepted by the vegetation canopy, and thus it is widely used for differentiating areas that contain healthy vegetation. We aim, in this paper, to characterize the phenology of vegetation through its NDVI profiles. To reach this goal, we propose, an approach based on sparse representation and dictionary learning. In literature, dictionary could be pre-designed or resulting from training process. The choice of which dictionary to use, is established according to the application context. In our work, we have chosen to con-

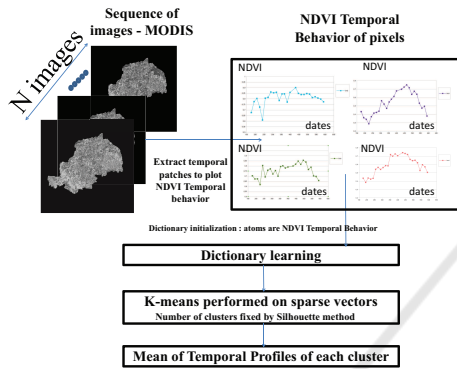


Figure 1: Proposed approach.

duct a dictionary learning process in order to fit the data and to characterize it only through its temporal behavior not through its spatial characteristics. Thus, in our case, we edit the K-SVD algorithm (Aharon et al., 2006) to do this learning: The first step is the dictionary initialization, we choose randomly samples from the study area which would be used as the atoms of dictionary. The design of the dictionary consists of two steps:

- **Sparse coding** where we determine the dictionary atoms' fitting given samples
- **Dictionary update** where we edit the atoms of dictionary in order to minimize approximation error.

In this paper, we propose an amelioration of the K-SVD algorithm consisting of substituting the OMP algorithm in sparse coding step, by the SunSAL algorithm. Thus, Algorithm 1 presents the usual K-SVD and Algorithm 2 presents its modification. We used them in our experimentation in order to compare their performance.

Since we don't have labeled data, we cannot determine the classes' labels of the samples using residual-based criterion of formula (4) described in previous section. Thus, we perform k-means algorithm to re-group signals having similar linear atoms combination into clusters. We vary the cluster's number in

Algorithm 1: Dictionary Design - K-SVD.

Data: Test Samples Y , initial dictionary D

Result: The learned dictionary D'

- **Sparse Coding** solving

$$\arg \min \|x\|_1 \text{ subject to } \|y - Dx\|_2 \leq \delta \quad (5)$$

- **Dictionary Update** minimize $E : E = Y - \sum d_j x_i$ using SVD, repeat until error E remains unchanged, where d_j is the j th atom of the dictionary and x_i is the i th element of a column of the sparse vector x .
-

Algorithm 2: Dictionary Design - K-SVD modified.

Data: Test Samples Y , initial dictionary D

Result: The learned dictionary D''

- **Sparse Coding** solving

$$\min \frac{1}{2} \|y - Dx\|_2^2 + \lambda \|x\|_1 \quad (6)$$

- **Dictionary Update** minimize $E : E = Y - \sum d_j x_i$ using SVD, repeat until error E remains unchanged, where d_j is the j th atom of the dictionary and x_i is the i th element of a column of the sparse vector x .
-

order to find which of them gives the best silhouette values (Rousseeuw, 1987). The silhouette value can be calculated for each point and represents a measure of similarity of a given point to the other points in its own cluster (intra cluster distance), compared to points belonging to other clusters (inter cluster distance). For the i^{th} point, S_i is defined as:

$$S_i = \frac{b_i - a_i}{\max(a_i, b_i)} \quad (7)$$

where a_i is the average distance from the i^{th} point to the other points in the same cluster as i , and b_i is the minimum average distance from the i^{th} point to points in a different cluster, minimized over clusters. S_i value varies from -1 to 1. High values indicate that a given point fits its own cluster and weakly matched to others. If we have many negative Silhouette values, this means that the clustering process has whether decomposed the samples in too many or few clusters. Whereas, if we get many positive Silhouette values, this means that the result of the clustering process is appropriate.

The following Algorithm 3 exhibits the unsupervised clustering process :

After running this algorithm, we compute the dis-

Algorithm 3: Unsupervised Clustering.

Data: Time series images T , learned dictionaries D' and D'' obtained from the previous algorithms

Result: Clusters of training samples

- **Step 1:** Extract randomly temporal samples from T and reconstruct it using OMP or SunSAL over respectively D' and D'' dictionaries
- **Step 2:** Calculate the Silhouette value of the sparse vectors resulting from the previous step, in order to determine the number of clusters
- **Step 3:** K means clustering algorithm on sparse vectors using the number of clusters found in step 2

criminant temporal behavior of each cluster which is the mean of all intra-cluster temporal behavior. This procedure helps us to reduce dimensionality since we conduct clustering process on sparse vectors instead of large signals. The Figure 1 exhibits an overview of the proposed approach.

4 STUDY AREA AND DATA

The study area corresponds to Taquari basin, located almost entirely in the state of Mato Grosso do Sul in the Center-West of Brazil - Figure 2.

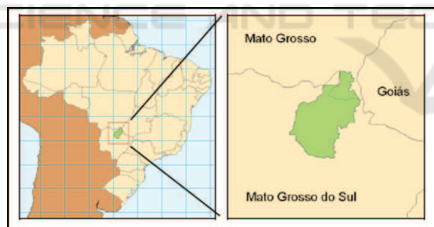


Figure 2: The state of Mato Grosso do Sul in the Center-West of Brazil.

We have a time-series data from MODIS-Terra satellite, "Vegetation Indices 16 days L3 Global 250 m" product which has two indices and ten other channels for each image: the NDVI and EVI (Enhanced Vegetation Index). We have used only the NDVI channel thanks to its relevance (Jonathan et al., 2005). The used time series contains 26 acquisitions, spanning a period from August 2000 to July 2001 which considered as significant to track vegetation evolution (complete phenology cycle). For the validation phase, we have a classification image at MODIS scale - Figure 3, elaborated from a Landsat image and expert validation. We have to emphasize that having a well documented study region is considered challenging.

Table 1: Silhouette values resulted from the variation of cluster number which are the input of kmeans algorithm. The data to be clustered are sparse vectors resulted from the two algorithms of Dictionary Learning: Algo1(K-SVD) and Algo2(K-SVD modified).

nb clus	DL:Algo1	DL:Algo2
1	NaN	NaN
2	0.5809	0.8489
3	0.3581	0.7364
4	0.2247	0.7331
5	0.1802	0.6881
6	0.1813	0.7059
7	0.1611	0.6208
8	0.1949	0.6792
9	0.1361	0.6287
10	0.1768	0.6589
11	0.1125	0.6529
12	0.1737	0.6694
13	0.1142	0.6623
14	0.1065	0.5945
15	0.0882	0.6521
20	0.1042	0.5400

5 EXPERIMENTAL PROTOCOL AND RESULTS

In this section, we evaluate the proposed approach by using MODIS time series data which contain 26 acquisitions. We focussed on the following parameters because they have a significant impact on the result:

- Since the temporal profiles of the pixels were noisy which could probably affect the final classification result, we proceeded to filter them by applying discrete wavelet transform (Daubechies functions)
- Dictionary: In order to consider all the possible types of vegetation, when creating our dictionary, we chose atoms from different regions that cover most of the studied area
- For the level of sparsity δ mentioned in equation (2), we varied δ empirically, until reaching a minimum value of MSE. This value was fixed to $\delta = 13$

This experiment is conducted on two dictionaries. The size of each one of them is 26×4868 where 26 is the number of dates, 4868 is the number of atoms. They are trained using both K-SVD and K-SVD modified algorithm as mentioned in Algorithm 1 and 2 respectively. Next, we run kmeans using different number of clusters : 1,2,3..to 20. To find out which is the

appropriate number, we calculate the silhouette value of each resulted cluster. This value indicates whether the cluster needs to be further divided or not. The results are illustrated in Table 1 showing silhouette values' variation according to the number of clusters. The lines correspond to the number of clusters used in kmeans, and columns correspond to the algorithm used to train the dictionary.

According to Table 1, the use of SunSAL as classifier, has led to better silhouette values. In fact, all the SunSAL's silhouette values are near to 1 which means we have a good segregation ratio. Here SunSAL suggests that the data could be divided in $k = 6$ clusters while OMP suggests that $k = 8$. Thanks to this table, we discard the classifier OMP because of its very low silhouette values and we keep SunSAL classifier since it grants better results. So with $k = 6$, we obtain 6 clusters where the mean profiles are represented in Figure 4. To evaluate our experimental result, we use a ground truth of the studied region described in (Jonathan et al., 2005) (Figure 3).

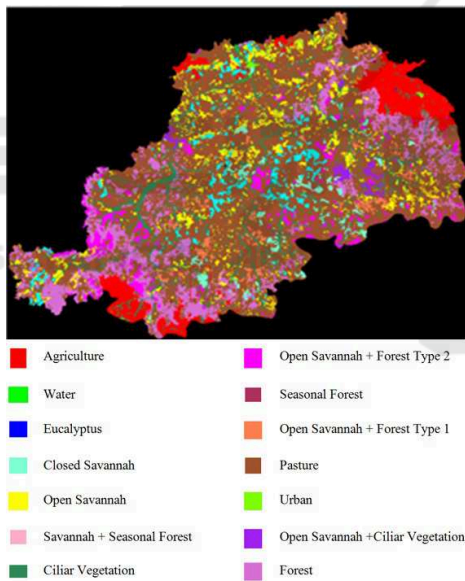


Figure 3: Reference Classes (Jonathan et al., 2005).

Our aim is to match the clusters found by kmeans to the classes of ground truth in order to identify the land cover types. So we calculate the Mean Square Error (MSE) between the estimated temporal behaviors and the reference classes. The Table 2 presents in columns the ground truth classes and in lines the label of clusters belonging to kmeans algorithm result. This table helps us finding the land cover types corresponding to clusters. For example, according to Table 2, cluster 2 corresponds to Ciliar Vegetation and Open Savannah, while cluster 6 corresponds to

Forest. This is confirmed in Figure 5 where we superpose the mean profile in cluster 2 with the mean of Ciliar Vegetation and Open Savannah. We have done the same thing to cluster 6 by superposing it with the Forest profile of ground truth in Figure 6.

Whereas cluster 5 is confused with several classes : Closed Savannah, Seasonal Forest and Open Savannah + Forest Type 1. This could be explained by the fact that those 3 classes have close temporal profiles and thus we could regroup all of them in a one single profile.

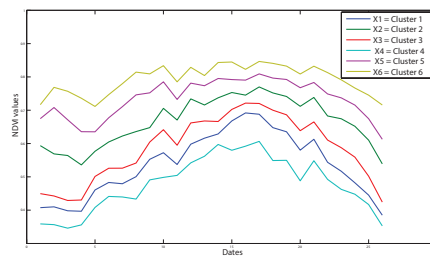


Figure 4: Mean profiles of the 6 found clusters.

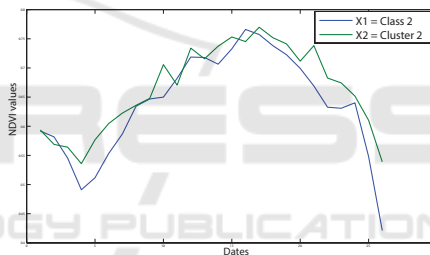


Figure 5: A: Superposition of Cluster 2 mean profile with the mean profile of Ciliar Vegetation and Open Savannah.

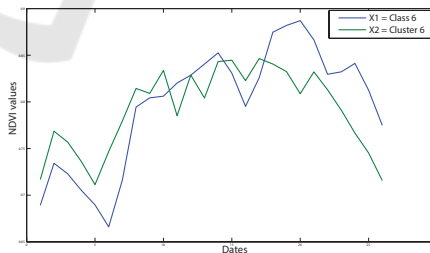


Figure 6: Superposition of Cluster 6 mean profile with the Forest profile.

So, thanks to our approach, we have found clusters that gather more than one ground truth classes. Table 3 shows matching result of our clusters with ground truth classes. By this way, based on information in Table 3, we can generate labeled dictionary by determining to which class, each atom belongs.

We succeed to identify the majority of classes, but we estimate that some of them are not well recognized

Table 2: Table 2 of MSE values of Sunsals classifier, where A=Argriculture, B=Water,C=Eucalyptus,D=Open Savannah, E=Closed Savannah, F=Forest, G=Seasonal Forest, H=Ciliar Vegetation I= Open Savanah+ciliar vegetation, J=Open Savanah+Forest type 1, K= Open Savanah+Forest type 2, L= Savannah+ Seasonal Forest, M=Pasture, N=Urban.

	A	B	C	D	E	F
1	0,013702123	0,014358648	0,00394132	0,014724775	0,045046558	0,072690414
2	0,043921584	0,022896723	0,031124566	0,002306937	0,007234252	0,019553144
3	0,020523329	0,016096906	0,010706222	0,007059779	0,026975737	0,049272183
4	0,01338676	0,017668488	0,002655275	0,029399763	0,072473686	0,105373549
5	0,076233369	0,042593683	0,060901952	0,009707884	0,001062428	0,005719512
6	0,110176038	0,065631921	0,09301972	0,023370714	0,004278307	0,001799481
	G	H	I	J	K	L
1	0,056415746	0,011683206	0,006053524	0,052763398	0,005628253	0,003442471
2	0,01302728	0,001776301	0,006218013	0,010195047	0,012103119	0,008181732
3	0,037179256	0,00419623	0,002892844	0,033783286	0,003984626	0,00177814
4	0,084818225	0,027074711	0,015296688	0,081290543	0,011946412	0,011910625
5	0,005061559	0,010941475	0,021002377	0,001024141	0,031136352	0,025381872
6	0,005089482	0,026979652	0,041094464	0,001690714	0,05498827	0,047385143
	M	N				
1	0,008173389	0,017284448				
2	0,004114109	0,066694088				
3	0,002740651	0,032219417				
4	0,020860182	0,005923803				
5	0,015761101	0,108046735				
6	0,033708819	0,149705802				

Table 3: New classes elaborated after conducting our approach.

Clusters	Ground truth classes
1	Water (B)
2	OpenSav and CiliarVeg (D+H)
3	OpenSav+CiliarVeg, Forest+OpenSav Type 2 and Sav+SeasonForest (I+K+L)
4	Agriculture, Eucalyptus and Urban (A,C,N)
5	OpenSav+Forest Type 1 and ClosedSav and SeasonForest (J+E+G)
6	Forest (F)

such as Agriculture. This deduction comes from the fact that its MSE is relatively high (0.013) and this can be explained by the heterogeneity of its class: it represents three behavior's types as illustrated in Figure 7 and (Jonathan et al., 2005).

6 CONCLUSION

Thanks to coarse data, we conducted a clustering process and generated "labeled" dictionary. We explored the sparse representation and its capabilities to fit the data, to reduce dimensions in order to improve clustering results. We compared two classifiers : OMP and SunSAL and found that SunSAL outperforms OMP. But here some critics must be mentioned : although MODIS images provide coverage at continental and global scales, the ability to reveal specific details of the region study remains difficult. Many of pixels generated by coarse resolution sensors are not characteristic of only one vegetation but represent a mixture as we mentioned in the experimentation section. Therefore, for this study, we consider that the pixel refers to one type of vegetation. So, in perspectives, we aim to accurate our results by finding a way to tradeoff multi-sensor data in order to enhance class discrimination to monitor land cover change. This would be done by the mean of merging multi-source images with different spatial, spectral and temporal resolutions.

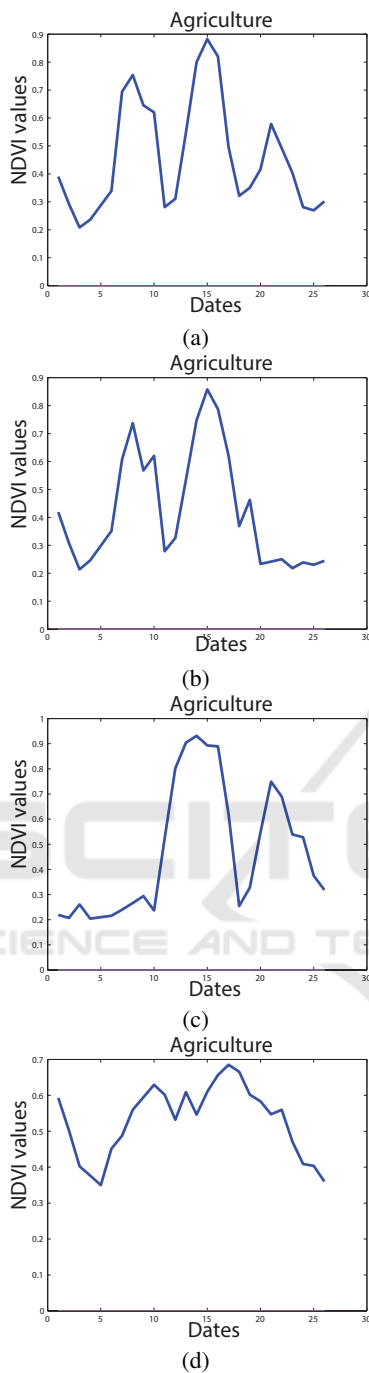


Figure 7: Ground truth temporal behaviors of Agriculture Class. (a): Agriculture Temporal Behavior with 3 modes. (b) and (c): Agriculture temporal behavior with 2 modes. (d) : Agriculture Temporal Behavior with 1 mode.

ACKNOWLEDGEMENTS

The authors would thank the anonymous reviewers for their helpful comments.

REFERENCES

- Aharon, M., Elad, M., and Bruckstein, A. (2006). K-svd: An algorithm for designing overcomplete dictionaries for sparse representation. *Signal Processing, IEEE Transactions on*, 54(11):4311–4322.
- Bioucas-Dias, J. M. and Figueiredo, M. A. (2010). Alternating direction algorithms for constrained sparse regression: Application to hyperspectral unmixing. In *Hyperspectral Image and Signal Processing: Evolution in Remote Sensing (WHISPERS), 2010 2nd Workshop on*, pages 1–4. IEEE.
- Brown, J. C., Kastens, J. H., Coutinho, A. C., de Castro Victoria, D., and Bishop, C. R. (2013). Classifying multiyear agricultural land use data from mato grosso using time-series modis vegetation index data. *Remote Sensing of Environment*, 130:39–50.
- Chen, S. and Donoho, D. (1994). Basis pursuit. In *Signals, Systems and Computers, 1994. 1994 Conference Record of the Twenty-Eighth Asilomar Conference on*, volume 1, pages 41–44. IEEE.
- Guha, T. and Ward, R. K. (2012). Learning sparse representations for human action recognition. *Pattern Analysis and Machine Intelligence, IEEE Transactions on*, 34(8):1576–1588.
- Jia, K., Wu, B., and Li, Q. (2013). Crop classification using hj satellite multispectral data in the north china plain. *Journal of Applied Remote Sensing*, 7(1):073576–073576.
- Jonathan, M., Meirelles, M. S. P., Berroir, J.-P., Herlin, I., and da Costa Coutinho, H. L. (2005). Regional scale land use/land cover classification using temporal series of modis data at the high taquari basin, ms, brazil. *Simpósio Brasileiro de Sensoriamento Remoto*, 12:579–581.
- Lim, Y., Shinn-Cunningham, B., and Gardner, T. J. (2012). Sparse contour representations of sound. *Signal Processing Letters, IEEE*, 19(10):684–687.
- Mahmoudi, M. and Sapiro, G. (2012). Sparse representations for range data restoration. *IEEE transactions on image processing: a publication of the IEEE Signal Processing Society*, 21(5):2909–2915.
- Mohammady, M., Moradi, H., Zeinivand, H., and Temme, A. (2015). A comparison of supervised, unsupervised and synthetic land use classification methods in the north of iran. *International Journal of Environmental Science and Technology*, 12(5):1515–1526.
- Morton, D. C., DeFries, R. S., Shimabukuro, Y. E., Anderson, L. O., Del Bon Espirito-Santo, F., Hansen, M., and Carroll, M. (2005). Rapid assessment of annual deforestation in the brazilian amazon using modis data. *Earth Interactions*, 9(8):1–22.
- Rousseeuw, P. J. (1987). Silhouettes: a graphical aid to the interpretation and validation of cluster analysis. *Journal of computational and applied mathematics*, 20:53–65.
- Tropp, J., Gilbert, A. C., et al. (2007). Signal recovery from random measurements via orthogonal matching pursuit. *Information Theory, IEEE Transactions on*, 53(12):4655–4666.

- Wright, J., Yang, A. Y., Ganesh, A., Sastry, S. S., and Ma, Y. (2009). Robust face recognition via sparse representation. *Pattern Analysis and Machine Intelligence, IEEE Transactions on*, 31(2):210–227.
- Xue, Z., Li, J., Cheng, L., and Du, P. (2015). Spectral-spatial classification of hyperspectral data via morphological component analysis-based image separation. *Geoscience and Remote Sensing, IEEE Transactions on*, 53(1):70–84.
- Yang, X., Yang, T., Ji, Q., He, Y., and Ghebregabher, M. G. (2014). Regional-scale grassland classification using moderate-resolution imaging spectrometer datasets based on multistep unsupervised classification and indices suitability analysis. *Journal of Applied Remote Sensing*, 8(1):083548–083548.
- Zhan, X., Sohlberg, R., Townshend, J., DiMiceli, C., Carroll, M., Eastman, J., Hansen, M., and DeFries, R. (2002). Detection of land cover changes using modis 250 m data. *Remote Sensing of Environment*, 83(1):336–350.

